Preparation, Characterization and Application of Nanospherical α-Fe_2O_3 Supported on Silica for Photocatalytic Degradation of Methylene Blue

Arastehnodeh, Ali
Chemical Engineering Department, Quchan Branch, Islamic Azad University, Quchan, I.R. IRAN

Saghi, Majid*[+]
Young Researchers and Elite Club, Arak Branch, Islamic Azad University, Arak, I.R. IRAN

Khazaei Nejad, Mohammad
Department of Chemistry, Mashhad Branch, Islamic Azad University, Mashhad, I.R. IRAN

ABSTRACT: *In the research, spherical α-Fe_2O_3 NanoParticles (NPs) were synthesized through Forced Hydrolysis and Reflux Condensation (FHRC) process and were supported on the surface of silica sand by Solid-State Dispersion (SSD) method. Characterization of silica and α-Fe_2O_3/SiO_2 catalyst was done using Fourier-Transform InfraRed (FT-IR) spectroscopy, Scanning Electron Microscopy (SEM) images, X-Ray Diffraction (XRD) patterns and Brunauer, Emmet and Teller (BET) surface area. The supported α-Fe_2O_3/SiO_2 nanocatalyst with the average crystallite size of 27.5 nm was used for photocatalytic removal of Methylene Blue (MB) from aqueous solutions under Ultra-Violet (UV) light. In order to optimization of effective parameters on MB degradation, the single-variable method was used. The optimal conditions were determined as pH=11, initial concentration of MB=10 ppm, and the mass of catalyst =1.0 g. Degradation efficiency in optimal conditions was 97.32%.*

KEYWORDS: *Methylene blue; SSD; FHRC; α-Fe_2O_3; SiO_2.*

INTRODUCTION

One of the most important concerns of environmentalists is the chemical pollutant penetration into the environmental cycle. These pollutants removal before their entrance into the environment is so significant since some pollutants have stable chemical structures may resistant for a long time in the environment and cause destructive consequences [1]. In the aqueous mediums, applying the advanced chemical methods for elimination of these pollutants is essential because the ordinary methods of refinery could not be used for complete elimination of chemicals [2]. Dyes regarding the great amount of production, consumption, and applications are a large group of chemical pollutants. MB is a colorcationic with molecular structure depicted in Fig. 1.

* *To whom correspondence should be addressed.*
+ E-mail: m-saghi@iau-arak.ac.ir
1021-9986/2019/2/21-28 8/$/5.08

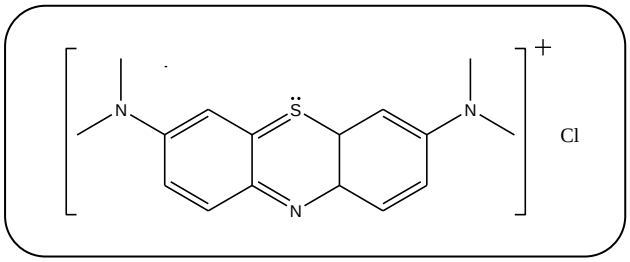

Fig. 1: Molecular structure of MB.

Inhalation of MB causes respiratory distress and direct exposure to eye and skin could cause severe damage and also could ends to nausea, sweating and mental disorders so that the effective removal of this dye from the water resources seems to be very important [3]. MB used as dye and indicator in different industries such as porcelain and ceramic companies. In porcelain companies, MB used as the detector that shows the defects such as dent, crack, and gap which occurs during the production process on the surface of porcelains. Without MB these defect could not be seen. For this propose, at first the produced items dyed by MB and after that examined visually. During this process, huge amount of MB enter to the wastewaters, environments and water resources. Hence, removal of this dye from wastewater through anyway is so important. Until now different chemical and physical methods such as adsorption and chemical decomposition were used for MB degradation in different mediums [4, 5]. One of the effective and sufficient methods for degradation of pollutants is the usage of Advanced Oxidation Processes (AOPs) [6]. Photocatalytic processes are so important AOPs in which semiconductors were used as catalyst. The catalyst is activated by receiving the energy of light and its electron from Valence Band (VB) transfer to Conduction Band (CB). The reason for creation of large amount of free radicals such as hydroxyl radicals ($OH^{\bullet}$) is this transfer. Hydroxyl radicals through attaching to the molecular structure of pollutant cause to the breaking the bonds and transferring to mineral species, H_2O and CO_2 [7]. CdS, PbS, GaS and ZnO are examples of photocatalysts which used for degradation of MB [8]. In this regard, Iron oxide can also be used.

Amongst different types of iron oxide, hematite with rhombohedral structure is one of the most common and widely used iron oxide. α-Fe_2O_3 has multiple applications which magnetic materials, gas sensors, data storages, pigments, catalysts, and photocatalysts are the most important ones [9]. In order to synthesis nano-Fe_2O_3, many different methods have been used among which sol-gel, co-precipitation, sonochemical synthesis, Micelle synthesis, hydrothermal synthesis, thermal decomposition, and FHRC are the most important methods [10-16]. In catalytic processes, wastewater treatments are of the most important α-Fe_2O_3 NPs applications. α-Fe_2O_3 NPs could be used in the form of a fine powder or crystals dispersed into water, but after the catalytic reaction, filtering step is so difficult. In order to solve this problem, researchers have examined methods for supporting α-Fe_2O_3 NPs on the surface of organic, inorganic or organic-inorganic materials [17, 18]. Different methods have been applied for supporting catalysts on the surface of catalyst support. One of these methods is SSD method in which catalyst precursor and catalyst support are mixed. Then during calcination, the catalyst is both formed and thermally supported on the surface of catalyst support [19].

So far, various methods and materials have been used to remove MB from a different environment, but the purpose of this project is to use the novel catalyst of α-Fe_2O_3/SiO_2 for the first time in order to effective degradation of MB. In this paper, spherical α-Fe_2O_3 NPs were supported on the surface of silica sand by using SSD method. The prepared α-Fe_2O_3/SiO_2 nanophotocatalyst was used for decomposition of MB pollutants under UV light. The effective parameters on the degradation process were optimized through single-variable method.

EXPERIMENTAL SECTION

Material and apparatuses

Iron (III) chloride hexahydrate, urea, methylene blue, sulfuric acid 96%, sodium hydroxide, and ethanol were provided by Merck Company. Also, silica sand (particle size < 0.04 μm) was purchased from Iranian company of Kimia Sadr (Yazd, Iran). Deionized water was used throughout the experiments and all the experimental tests are performed at room temperature. The FT-IR spectra, Surface morphology and X-ray diffraction patterns of silica and α-Fe_2O_3/SiO_2 were done using a Perkin-Elmer spectrophotometer (Spectrum Two, model), a Philips XL-30 SEM and a DX27-mini diffractometer, respectively. BET surface area of materials was determined by N_2 adsorption-desorption

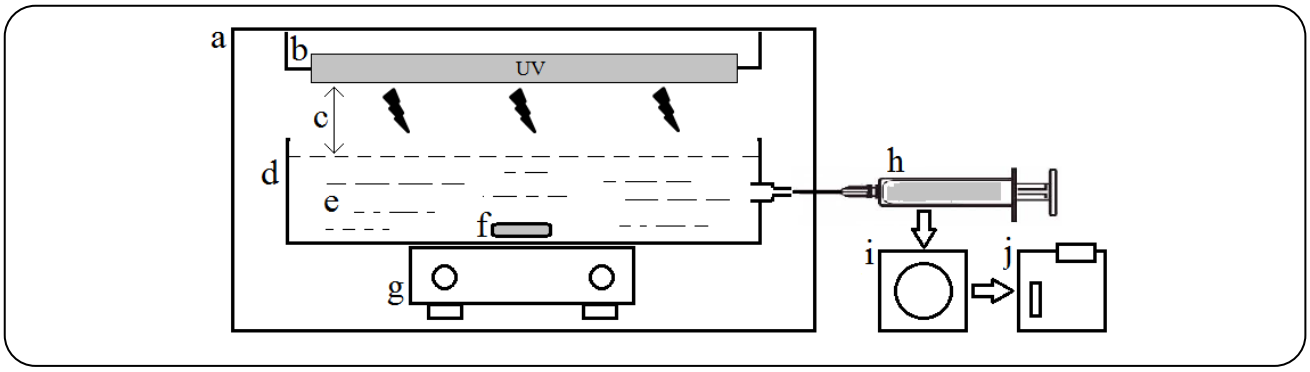

Fig. 2: Schematic diagram of photocatalytic reactor. (a) MDF box; (b) UV lamps (Philips; 15W, 360 mA); (c) The distance between the surface of MB solution and lamps, 5 cm; (d) Reactor, 300 mL capacity; (e) MB solution, 250 mL; (f) Magnet; (g) Magnetic stirrer; (h) Sampling port; (i) Centrifuge; (j) UV/Vis spectrophotometer.

the method at 77 K, measured using a BELSORP-mini II instrument. All UV/Vis absorption spectra were obtained using an Agilent 8453 spectrophotometer.

Synthesis of α-Fe_2O_3 NPs

According to Bharathi et al. [16], firstly 100 mL iron (III) chloride hexahydrate 0.25 M was poured into a flat-bottom flask. When the Iron solution was agitated by stirrer, it was added drop by drop to it 100 mL urea 1 M. The obtained mixture was stirred for 30 min and then placed under the reflex at 90–95 °C for 12 h. Then, the precipitate was washed with deionized water because unreacted ions will be removed. The washed precipitate was dried at 70 °C for 2 h. Having fully dried, one light brown solid (iron hydroxide) was yielded. Finally, this solid remained at 300 °C for 1 h; hence the iron hydroxide particles will transform to iron oxide. Consequently, a dark brown solid of α-Fe_2O_3 was obtained.

Preparation of α-Fe_2O_3/SiO_2 catalyst (SSD method)

According to Nikazar et al. [19], the synthesized iron hydroxide (the middle product of α-Fe_2O_3 NPs procedure) and SiO_2 catalyst support were mixed with a weight ratio of 1:3 (weight of SiO_2 is three times of α-Fe_2O_3) using an agate pestle and mortar for 1 h. To have better mixture, ethanol was sprayed on the mixture until it becomes doughform. The resulted mixture was dried kept at 80 °C for 2 h. To do calcination and transform iron hydroxide particles fixed on the surface of Silica into α-Fe_2O_3, the obtained solid was kept at 300 °C for 1 h.

General procedure

Fig. 2 shows one schematic of the photocatalytic reactor used in the study. On the upper section of the box, two mercury lamps were built-in as UV light sources. The radiation is generated almost exclusively at 254 nm. The solution inside the reactor was agitated by magnetic stirrer. In each of the experiments, firstly 250 mL MB solution was made as specified concentration and poured inside the reactor. Then, at related pH, the specified amount of α-Fe_2O_3/SiO_2 catalyst was added to the solution inside the reactor. In all experiments, pH adjustment was done via minimum use of H_2SO_4 and NaOH. Then, stirrer and UV lamps were immediately turned on to initiate the process. Sampling was done by a 5 ml syringe, every 30 min. In order to fully separate the catalyst from solution, the samples were centrifuged for 3 min with 3500 rpm speed. The MB concentration of the solutions was determined at λ_{max}=660 nm. The percentage of photodegradation efficiency (x%) as a function of time is given by

$$x\% = \frac{C_0 - C}{C_0} \times 100 \quad (1)$$

Where C_0 and C are the concentration of MB (ppm) at t=0 and t at any time, respectively. In the experiments, the initial concentration of MB varied from 10 to 20 ppm at five levels (10, 12.5, 15, 17.5 and 20 ppm), pH varied from 3 to 11 at five levels (3, 5, 7, 9 and 11) and catalyst mass varied from 0.2 to 1.0 gram at five levels (0.2, 0.4, 0.6, 0.8 and 1.0 g).

RESULTS AND DISCUSSION

Characterization

SEM images of silica sand and prepared α-Fe_2O_3/SiO_2 catalyst are shown in Fig. 3 and Fig. 4, respectively. Fig. 4 indicates that α-Fe_2O_3 particles were spherical and uniformly supported on the surface of SiO_2.

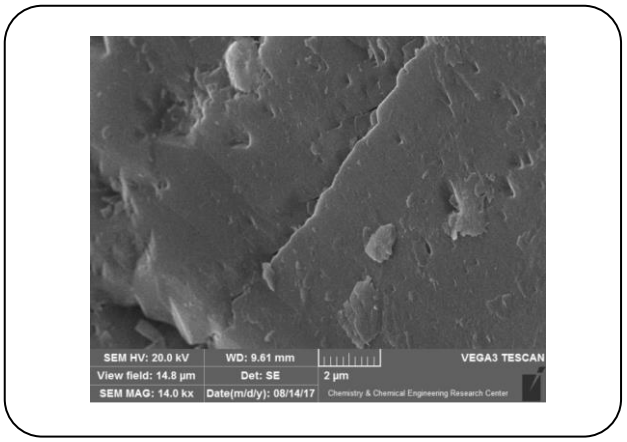

Fig. 3: SEM image of silica sand (SiO_2).

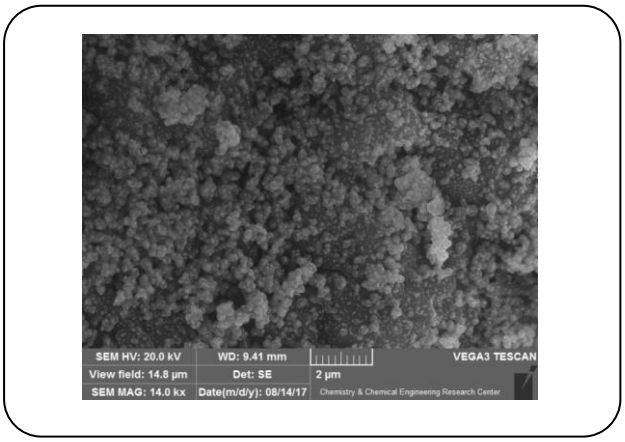

Fig. 4: SEM image of α-Fe_2O_3/SiO_2 catalyst.

In Figs. 5a and 5b, FT-IR spectra of silica and α-Fe_2O_3/SiO_2 have been shown, respectively. As can be seen, in spectrum 5a in addition to the silica's specific peaks belong to the vibrations of SiO_2 and Si-OH, a weak peak of iron appeared as a reason of a few quantities of iron in the structure of mineral silica. Also, in Fig. 5b, it is clear that absorption peaks of SiO_2 have appeared without considerable change in the wave numbers; only their intensities have been slightly changed. It means that SiO_2 was stable and it had not been changed chemically during preparing α-Fe_2O_3/SiO_2. Also, characteristic peaks of α-Fe_2O_3 have well appeared and are in agreement with *Bharati et al.* [16]. These characteristic peaks which are related to stretching and bending modes of OH and Fe–O binding in FeOOH, in some cases overlapped with absorption peaks of SiO_2. In FTIR spectrum Fig. 5a, appearance of related peak to Fe-O vibrational mode indicates the existence of a few percent irons in the silica sand structure. Since the used silica sand in this paper in not high purity grade (industrial grade), existence of such peaks that related to some other elements except Si is normal.

In Fig. 6a and 6b, XRD patterns of silica and α-Fe_2O_3/SiO_2 have been illustrated, respectively. In both these patterns, silica-specified peaks have well appeared which indicate that silica sand was stable during the supporting process in SSD method. In these patterns, α-Fe_2O_3-specified peaks that have also been marked have appeared and it is in agree with results of *Bharati et al.* [16]. The warren-averbach analysis method is an appropriate method for extraction of nanostructure data's from the XRD pattern, through which the average crystal's sizes could be calculated. This theory is attributed to B. E. Warren and B. L. Averbach and has become accepted as one of the more rigorous and widely used methods for separating the effects of size and strain [20]. Taking account of device errors, the crystallite size of spherical α-Fe_2O_3 supported on the surface of silica was calculated by using XRD and Warren-Averbach theory that their average was 27.5 nm.

The BET surface area of materials was measured by N_2 adsorption-desorption method at 77 K. The samples were degassed under vacuum at 473 K for 12 h before the BET measurement. The BET surface area of silica and α-Fe_2O_3/SiO_2 were determined 18.33 and 61.45 (m^2/g), respectively. The results show that the Fe supporting on the surface of SiO_2 caused the increasing of catalysts surface area to about 3 times, therefore, it improves the catalyst performance because of increasing the surface area, the number of available active sites for chemical reaction increased.

UV/Vis test of MB

Fig. 7 shows the absorbance spectrum related to one of the MB samples versus wavelength at the beginning of reaction (t=0) and after 15, 30, 45, 60, 75, 90, 105 and 120 minutes of photocatalytic reaction (from top to bottom). In order to determination of MB concentration at any time and calculation of degradation percentage (x%) using equation (1), it's absorbance at λ_{max} = 660 nm considered.

Photocatalytic mechanism

When α-Fe_2O_3 supported on the surface of silica is illuminated by UV light, electrons are promoted from

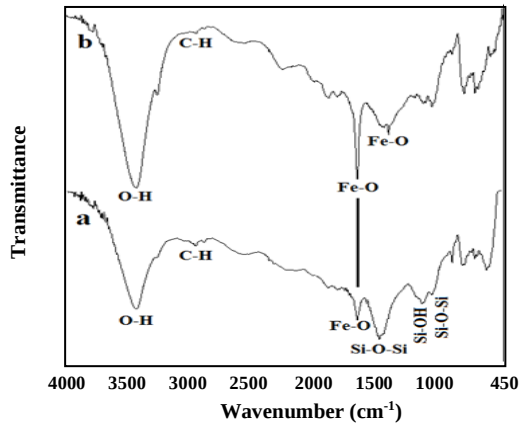

Fig. 5: FT-IR spectra of Silica sand (a) and α-Fe_2O_3/SiO_2 catalyst (b).

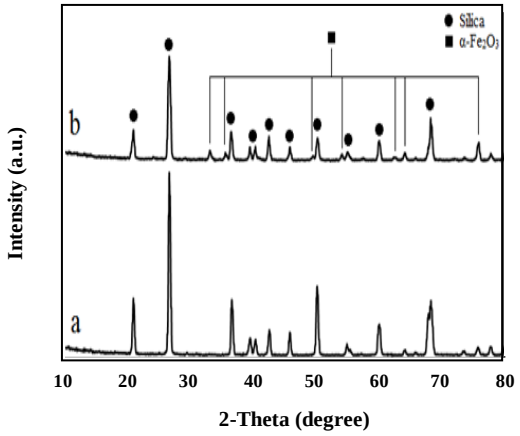

Fig. 6: X-ray diffractogram of Silica sand (a) and α-Fe_2O_3/SiO_2 catalyst (b).

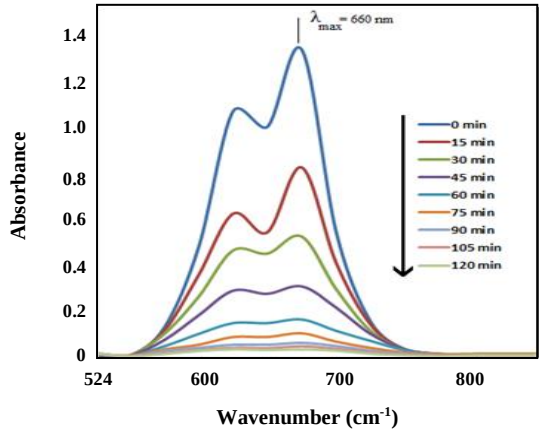

Fig. 7: UV/Vis spectral absorption changes of MB solution photodegraded by α-Fe_2O_3/SiO_2.

the VB to the CB of the semiconductor to give electron-hole pairs. The VB potential (h_{VB}) is positive enough to generate hydroxyl radicals at the surface, and the CB potential (e_{CB}) is negative enough to reduce molecular oxygen. The hydroxyl radical is a powerful oxidizing agent and attacks MB molecules present at or near the surface of α-Fe_2O_3. It causes the photo-oxidation of MB according to the following reactions:

$$Fe_2O_3 \xrightarrow{hv} Fe_2O_3\left(e^-_{CB} + e^+_{VB}\right)$$

$$h^+_{VB} \xrightarrow{H_2O_{(ads)}} H^+ + {}^{\bullet}OH^-_{(ads)}$$

$$h^+_{VB} \xrightarrow{OH^-_{(ads)}} {}^{\bullet}OH^-_{(ads)}$$

$$e^-_{CB} \xrightarrow{O_{2\ (ads)}} {}^{\bullet}O^-_{2\,(ads)}$$

$$H_2O \leftrightarrow H^+ + OH^-$$

$$O^-_{2\,(ads)} \xrightarrow{H^+} {}^{\bullet}HO_2$$

$$O^-_{2\,(ads)} \xrightarrow{H^+} {}^{\bullet}HO_2$$

$${}^{\bullet}HO_2 \xrightarrow{HO_2} H_2O_2 + O_2$$

$$H_2O_2 \xrightarrow{Fe_2O_3\left(e^-_{CB}\right)} OH + OH^- + Fe_2O_3$$

$${}^{\bullet}OH_{(ads)} \xrightarrow{MB} \text{Degradation of MB}$$

$$h^+_{VB} \xrightarrow{MB} \text{Oxidation of MB}$$

Fig. 8 shows the MB photocatalytic degradation pathway. The color of MB solutions becomes weaker when part of the methyl groups degrade and finally MB depredated into H_2O and CO_2 and other inorganic molecules [21].

The effect of MB initial Concentration on x%

In order to investigate the effect of MB initial concentration on the percent of MB photocatalytic degradation (x%), 5 samples of MB with different concentrations including 10, 12.5, 15, 17.5 and 20 ppm were prepped and then tested at pH=7 with catalyst concentration=0.6 g. Sampling through the reactor did each 15 minutes. Fig. 9 shows the diagram x% versus time for different initial concentration of MB. This diagram indicates that under the condition in which pH=7 and catalyst mass=0.6 g, the maximum value of x% achieved while the initial concentration of MB is 10 ppm. The UV light can be made to go more easily through the solution

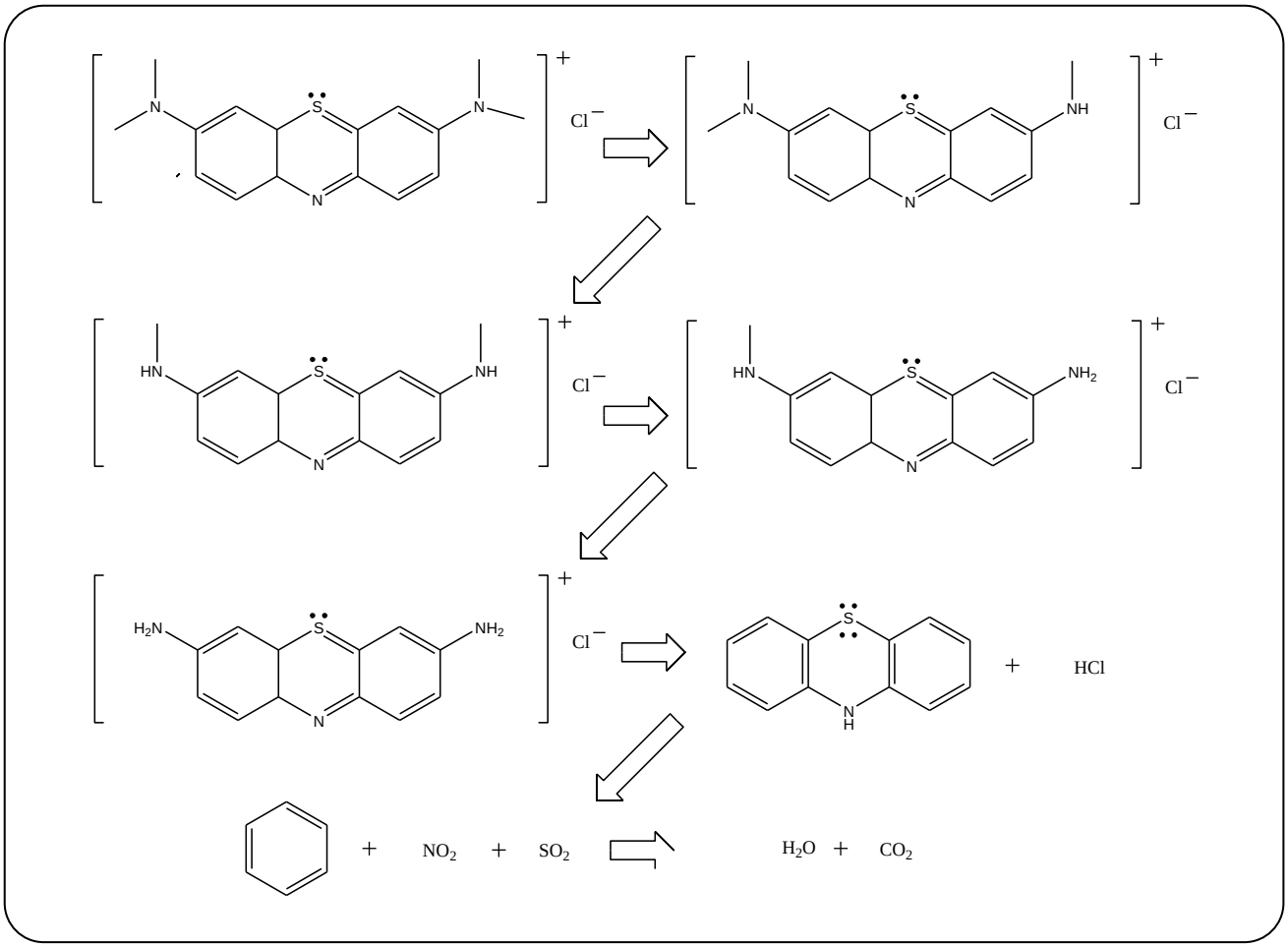

Fig. 8: Photocatalytic degradation pathway of MB.

to irradiate the α-Fe_2O_3/SiO_2 when the initial concentration of MB is lower, hence, photocatalytic efficiency increased with decreasing initial concentration of MB.

The effect of pH on x%

The pH effect on the x% with consideration of MB initial concentration=15 ppm and catalyst mass=0.6 g was investigated. For this purpose, 5 samples with pH values of 3, 5, 7, 9 and 11 prepared. Fig. 10 shows the diagram x% versus time for different pH. The results of this diagram show that under the prevailing conditions, the maximum of x% was obtained at pH=11. Because MB is a cationic color and surface of α-Fe_2O_3 particles at alkali solutions get negative charge, hence, cationic species such as MB molecules can be easily adsorbed on the surface of photocatalyst. Therefore photocatalytic degradation of MB dye is done better at basic conditions.

The effect of α-Fe_2O_3/SiO_2 mass on x%

Regarding the results of two previous diagrams, in order to investigation of catalyst mass effect on x%, various masses of α-Fe_2O_3/SiO_2 catalysts including 0.2, 0.4, 0.6, 0.8 and 1.0 gram were tested under the pH=11 and initial concentration of MB=10 ppm condition. Fig. 11 shows the diagram x% versus time for different catalyst masses. This diagram shows that the maximum degradation of MB (97.32) obtained in the presence of 1.0 g α-Fe_2O_3/SiO_2 catalyst under above mentioned condition. By increasing the catalyst amount, the number of free electrons in CB increased and these free electrons generate more free radicals. Therefore, increasing the catalyst's mass increases x%. Of course it should be noted that excessive increasing of catalyst rather than optimum value cause some problems such as cost increase or the filtering difficulties after reaction and pollutant degradation.

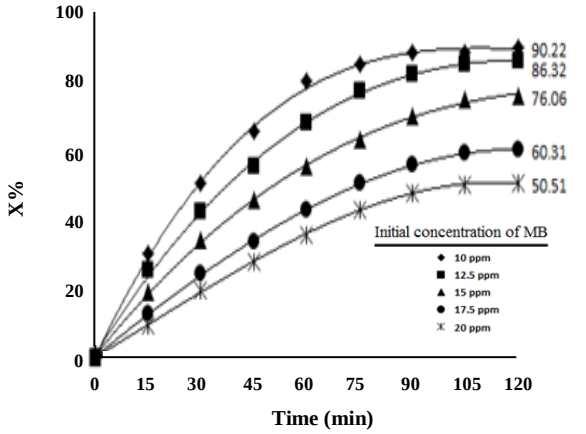

Fig. 9: The effect of MB initial concentration on x% (pH=7, Catalyst Mass=0.6 g).

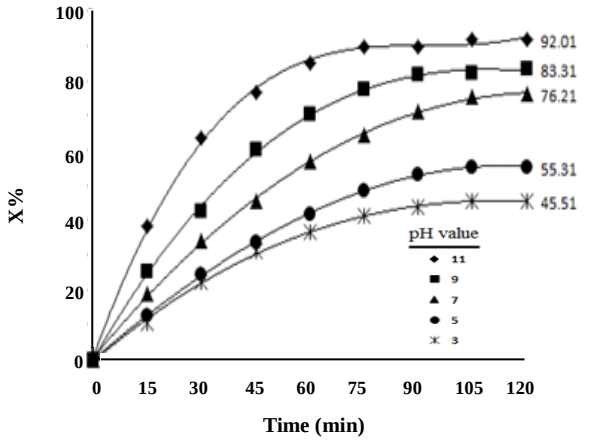

Fig. 10: The effect of pH on x% (initial concentration of MB=15 ppm, Catalyst mass=0.6 g).

CONCLUSIONS

In the study, spherical α-Fe_2O_3 nanoparticles of average crystallite size 27.5 nm were successfully synthesized by FHRC method meanwhile supported on the surface of silica sand through SSD approach. The prepared α-Fe_2O_3/SiO_2 was then utilized as a nanocatalyst for the photodegradation of MB dye as an organic pollutant under UV irradiation. In this paper, the effective parameters on the photodegradation process were investigated through single-variable system. At optimal conditions including pH=11, initial concentration of MB=10 ppm, and the mass of catalyst =1.0 g, the degradation efficiency was 97.32%.

Acknowledgement

The authors are grateful to the Maghsoud factories group for the financial support for this work.

Received : Sep. 25, 2017 ; Accepted : Feb. 26, 2018

REFERENCES

[1] Pourbabaee A. A., Malekzadeh F., Sarbolouki M. N., Mohajeri A., Decolorization of Methyl Orange (As a Model Azo Dye) by the Newly Discovered Bacillus Sp, *Iran. J. Chem. Chem. Eng. (IJCCE)*, **24**(3): 41-45 (2005).

[2] Fernandez C., Larrechi M. S., Callao M. P., An Analytical Overview of Processes for Removing Organic Dyes From Wastewater Effluents, *TrAC, Trends Anal. Chem.*, **29**(10): 1202-1211 (1020).

[3] Kirov M.Y., Evgenov O.V., Evgenov N.V., Egorina E.M., Sovershaev M.A., Sveinbjørnsson B., Nedashkovsky E.V., Bjertnaes L.J., Infusion of Methylene Blue in Human Septic Shock: A Pilot, Randomized, Controlled Study, *Crit. Care. Med.*, **29**(10): 1860-1867 (2001).

[4] Kavitha D., Namasivayam C., Experimental and Kinetic Studies on Methylene Blue Adsorption by Coir Pith Carbon, *Bioresour. Technol.*, **98**(1): 14-21 (2007).

[5] Umebayashi T., Yamaki T., Tanaka S., Asai K., Visible Light-Induced Degradation of Methylene Blue on S-Doped TiO_2, *Chemistry Letters*., **32**(4): 364-365 (2003).

[6] Dutta K., Mukhopadhyay S., Bhattacharjee S., Chaudhuri B., Chemical Oxidation of Methylene Blue Using a Fenton-like Reaction, *J. Hazard. Mater.*, **84**(1): 57-71 (2001).

[7] Taghavi K., Purkareim S., Pendashteh A. R., Chaibakhsh N., Optimized Removal of Sodium Dodecylbenzenesulfonate by Fenton-Like Oxidation Using Response Surface Methodology, *Iran. J. Chem. Chem. Eng. (IJCCE)*, **35**(4): 113-124 (2016).

[8] Dariani R. S., Esmaeili A., Mortezaali A., Dehghanpour S., Photocatalytic Reaction and Degradation of Methylene Blue on TiO_2 Nano-Sized Particles, *Optik-International Journal for Light and Electron Optics*, **127**(18): 7143-7154 (1016).

[9] Saghi M., Mahanpoor K., Photocatalytic Degradation of Tetracycline Aqueous Solutions by Nanospherical α-Fe_2O_3 Supported on 12-Tungstosilicic Acid as Catalyst: Using Full Factorial Experimental Design, *Int. J. Ind. Chem.*, **8**(3): 297-313 (2017).

[10] Farahmandjou M., Soflaee F., Synthesis and Characterization of α-Fe_2O_3 Nanoparticles by Simple Co-Precipitation Method, *Phys. Chem. Res.*, **3**(3): 191-196 (2015).

[11] Liang H., Liu K., Ni Y., Synthesis of Mesoporous α-Fe_2O_3 via Sol–Gel Methods Using Cellulose Nano-Crystals (CNC) as Template and its Photo-Catalytic Properties, *Mater. Lett*., **159**: 218-220 (2015).

[12] Diab M., Mokari T., Thermal Decomposition Approach for the Formation of α-Fe_2O_3 Mesoporous Photoanodes and an α-Fe_2O_3/CoO Hybrid Structure for Enhanced Water Oxidation, *Inorg. Chem*., **53**(4): 2304-2309 (2014).

[13] Jiang T., Poyraz A. S., Iyer A., Zhang Y., Luo Z., Zhong W., Miao R., El-Sawy A.M., Guild C.J., Sun Y., Kriz D.A., Suib S.L., Synthesis of Mesoporous Iron Oxides by an Inverse Micelle Method and Their Application in the Degradation of Orange II Under Visible Light at Neutral pH, *J. Phys. Chem. C.*, **119**(19): 10454-10468 (2015).

[14] Askarinejad A., Bagherzadeh M., Morsali A., Sonochemical Fabrication and Catalytic Properties of α-Fe_2O_3 Nanoparticles, *J. Exp. Nanosci*., **6**(3): 217-225 (2011).

[15] Tadic M., Panjan M., Damnjanovic V., Milosevic I., Magnetic Properties of Hematite (α-Fe_2O_3) Nanoparticles Prepared by Hydrothermal Synthesis Method, *Appl. Surf. Sci*., **320**: 183-187 (2014).

[16] Bharathi S., Nataraj D., Mangalaraj D., Masuda Y., Senthil K., Yong K., Highly Mesoporous α-Fe_2O_3 Nanostructures: Preparation, Characterization and Improved Photocatalytic Performance Towards Rhodamine B (RhB), *J. Phys. D: Appl. Phys*., **43**: 1-9 (2010).

[17] Chen M., Liu J., Chao D., Wang J., Yin J., Lin J., Fan H.J., Shen Z.X., Porous α-Fe_2O_3 Nanorods Supported on Carbon Nanotubes Graphene Foam as Superior Anode for Lithium Ion Batteries, *Nano Energy*., **9**: 364–372 (2014).

[18] Rancourt D. G., Julian S. R., Daniels J. M., Mossbauer Characterization of Very Small Superparamagnetic Particles; Application to Intra-Zeolitic α-Fe_2O_3 Particles, *J. Magn. Magn. Mater*., **49**(3): 305–316 (1985).

[19] Nikazar M., Gholivand K., Mahanpoor K., Photocatalytic Degradation of Azo Dye Acid Red 114 in Water with TiO_2 Supported on Clinoptililite as a Catalyst, *Desalination*., **219**(1-3): 293-300 (2008).

[20] Warren B. E., Averbach B. L., The Effect of Cold-Work Distortion on X-Ray Patterns, *J. Appl. Phys*., **21**(6): 595-599 (1950)

[21] Zhang T.Y., Oyama T., Aoshima A., Hidaka H., Zhao J.C., Serpone N., Photooxidative N-Demethylation of Methylene Blue in Aqueous TiO_2 Dispersions under UV Irradiation, *J. Photochem. Photobiol. A.*, **140**(2): 163-172 (2001).